

Non-linear electrical response
in a non-charge-ordered manganite : $\text{Pr}_{0.8}\text{Ca}_{0.2}\text{MnO}_3$

S. Mercone, A. Wahl*, Ch. Simon, C. Martin

*Laboratoire CRISMAT, Unité Mixte de Recherches 6508, Institut des
Sciences de la Matière et du Rayonnement - Université de Caen, 6*

Boulevard du

Maréchal Juin, 14050 Caen Cedex, France.

(November 2, 2018)

Abstract

Up to now, electric field induced non-linear conduction in the $\text{Pr}_{1-x}\text{Ca}_x\text{MnO}_3$ system has been ascribed to a current-induced destabilization of the charge ordered phase. However, for $x \leq 0.25$, a ferromagnetic insulator state is observed and charge-ordering is absent whatever the temperature. A systematic investigation of the non-linear transport in the ferromagnetic insulator $\text{Pr}_{0.8}\text{Ca}_{0.2}\text{MnO}_3$ shows rather similar results to those obtained in charge ordered systems. However, the experimental features observed in $\text{Pr}_{0.8}\text{Ca}_{0.2}\text{MnO}_3$ are distinct in that the collapse of the CO energy gap can not be invoked as usually done in the other members of the PCMO system. We propose interpretations in which the effectiveness of the DE is restored upon application of electric field.

Hole-doped perovskite manganese oxides $R_{1-x}AE_xMnO_3$ (R and AE, being trivalent rare-earth and divalent ions, respectively) are associated with a wide variety of electronic and magnetic properties depending on the value of x and the averaged A -site cation radius, $\langle r_A \rangle$.¹ These materials have recently been the subject of intense studies due to intriguing phenomena such as charge/orbital ordering (CO)² or colossal magnetoresistance (CMR).³ The latter is usually interpreted by means of the double-exchange interaction (DE) scenario⁴ which gives an interesting qualitative interpretation of coupled ferromagnetic ordering and metallicity. Within such a framework, the ferromagnetic (FM) ordering is related to a large electronic itinerancy i.e. metallic behavior. Among the various mixed valent manganites studied so far, the $Pr_{1-x}Ca_xMnO_3$ system (PCMO) is perhaps the most interesting because it shows a great variety of ordered phases very sensitive to cation / anion doping.⁵⁻¹¹ For $0.3 \leq x < 0.8$, charge ordering of Mn^{3+} and Mn^{4+} (CO) is found and an antiferromagnetic (AFM) ordering can be observed with Néel temperature ranging from 100K to 170K for $x = 0.8$ and 0.3, respectively. Due to its low tolerance factor, this system happens to remain insulating giving rise, under zero field, to a charge ordered insulating state (COI). It has been widely shown that this COI state in the PCMO system can be melted into a metallic ferromagnet (FMM) upon application of a magnetic field of sufficient amplitude.^{6,8,12-15} Within the doping range $0.3 \leq x \leq 0.5$, in addition to the magnetic field, such a destabilization of the COI state can also be induced by external perturbations such as irradiation by X-ray¹⁶ or light^{17,18} and application of pressure¹⁹ or electric field.²⁰⁻²⁵ Those optical or irradiation induced transitions are usually argued to be a result of classical percolation transport in a non-homogeneous medium ; however, the role of the application of electric field is not so clear.

For instance, Guha et al.^{22,23} found that the current induced destabilization of the COI state in $Pr_{0.63}Ca_{0.37}MnO_3$ leads to a regime of negative differential resistivity (NDR) ($\frac{dV}{dI} < 0$) with a concomitant enhancement of magnetization. The authors invoke the creation of low-resistivity conducting paths made up of FM phase along the current flow. Very recently, Yuzhelevski et al.²⁶ have claimed in low doped LCMO system that the influence of light, X-

ray and current may be interpreted in terms of spin-polarized tunnel conduction mechanism modifying phase separation-conditions along the percolation path.

Up to now, all experiments investigating the effect of electric field on the conducting behavior of the PCMO system have mostly been carried out on CO candidates. Consequently, interpretations based on multiphase coexistence (AF-COI and FMM phases whose respective volumes in the bulk are modified under perturbations) is often raised.^{17,18,20–23} The very low doping regime of the PCMO system has not been explored yet. For $x \leq 0.25$, a ferromagnetic insulator (FMI) state is found and charge-ordering is not observed whatever the temperature. Moreover, a metallic state is never realized, even upon application of a magnetic field. This can be understood as follows : on the one hand, for this system, we have an important inward tilt of the $Mn^{3+} - O - Mn^{4+}$ bonds which results in a decrease of the $d_{z^2} - p\sigma - d_{z^2}$ overlaps. This produces a decrease of the magnitude of the e_g bandwidth and, consequently, in a reduction in the effectiveness of the double exchange. On the other hand, for $x \leq 0.25$ we deal with a very low hole concentration which does not favor a delocalized electronic state.

The aim of our experience was to investigate whether a current-induced metal-insulator transition can be observed in a non-CO manganite of the PCMO system. For this purpose, a crystal of $Pr_{0.8}Ca_{0.2}MnO_3$, not so far from the CO region, has been chosen. Although a M-I transition has not been clearly observed, the resistance for increasing bias current is drastically reduced. Moreover, strong non-linear electrical conduction is found with a NDR developing for $T < T_c$. This behavior is not sensitive upon application of a magnetic field. Compared to already reported results, the experimental features observed here are distinct in that the collapse of the CO energy gap can not be invoke as usually done in the other members of the PCMO system.^{17,18,20–25}

Using the floating-zone method with a feeding rod of nominal composition $Pr_{0.8}Ca_{0.2}MnO_3$, a several-cm-long single crystal was grown in a mirror furnace. Two samples were cut out of the central part of this crystal, one of them for resistivity measurements and the other for magnetization and specific heat measurements. X-ray diffraction and

electron diffraction studies, which were performed on pieces coming from the same part of the crystal, attested that the samples are single phased, and well crystallized. The cell is orthorhombic with a $Pnma$ space group, in agreement with previously reported structural data. The energy dispersive spectroscopy analyses confirm that the composition is homogeneous and close to the nominal one, in the limit of the accuracy of the technique. The electron diffraction characterization was also carried out versus temperature, from room temperature to 90K. The reconstruction of the reciprocal space showed that the cell parameters and symmetry remain unchanged in the whole domain of temperature and, more especially, no extra reflections have been detected. This electron diffraction observation, coupled with lattice imaging, shows that, in our sample there is no charge ordering effect, even at short range distances. All X-ray and electron diffraction observations agree with previous published results for compounds of the same system.¹¹

In order to characterize the magnetic structure of the sample, we have performed a temperature dependence of the diffraction patterns on the $G4.1$ neutron spectrometer ($\lambda = 0.2426 \text{ nm}$) of the Orphee source (LLB-Saclay, France) in the 2θ angular range (2.00 - 81.90). The sample was first powdered and the diffracted spectra were recorded as function of temperature from 300K down to 1.5K. For $T < T_c$, the data were fitted with a $Pnma$ structure with a ferromagnetic order with the Mn spins aligned along the a axis and a resolution limited correlation length (more than 100nm). The saturated moment is 3.46(4) μ_B/Mn at 1.5K and the Curie temperature is around 135K. No evidence of any antiferromagnetic peak was observed in this sample down to 1.5K. The 1.5K experimental and calculated patterns given in Figure 1 test the validity of the fit. The 020 peak intensity versus temperature (see inset) shows the FM component evolution and allows T_c determination. A magnetic contribution was also added for Pr in the calculation at lower temperatures.

Four linear contact pads of In were soldered onto the sample in linear four-probe configuration. $V - I$ data were taken with current biasing (Keithley 236) and with a temperature control of 100 mK. The measurements under magnetic field were done using a superconducting magnet capable of producing 9 Tesla.

In Figure 2, we show the temperature variation of the resistance ($R = \frac{V}{I}$) of a $\text{Pr}_{0.8}\text{Ca}_{0.2}\text{MnO}_3$ crystal for various bias current, $R_I(T)$, under zero field. When the current is small ($10^{-3}mA$ et $1mA$), the sample shows an insulating behavior and, at low temperature, the large resistance increase overloads our current source. Our current source overloads for $100V$, thus the maximum resistance that we can measure for $10^{-3}mA$ is around $100M\Omega$. For higher currents ($10mA$ et $50mA$), the resistance is strongly depressed with a trend to saturation when the temperature is lowered. We do not see a clear metal-like decrease in resistance below T_c and the observed behavior is rather similar to that of $\text{Gd}_{0.5}\text{Ca}_{0.5}\text{MnO}_3$ and $\text{Nd}_{0.5}\text{Ca}_{0.5}\text{MnO}_3$ films deposited on LAO²⁴ and PCMO crystals.^{22,23} The latter papers report that electrical current triggers the collapse of the low temperature electrically insulating CO state to a FMM state. Measurements of $R_I(T)$ have been carried out upon cooling and warming and no hysteresis has been observed. Around $50K$, a slight anomaly can be observed on every $R_I(T)$, this can be linked to the Pr magnetic ordering as observed by neutron experiments.

Figure 3 shows $V - I$ characteristics in a semi-log scale for $T < T_c$ ($80K$, $90K$ and $100K$) under zero field. The $V - I$ characteristics for temperatures above the Curie temperature ($170K$ and $300K$) are displayed in Figure 4. For $T = 300K$, an ohmic conduction is observed on the whole current range. As one approaches T_c , non-linear conduction sets in. As T is lowered below T_c the non-linearity increases and the $V - I$ curves exhibit a negative differential resistance (NDR). The region of NDR is observed when the bias current attains a current threshold (I_{th}). The latter is higher when the temperature is close to T_c from below ($0.4mA$ at $80K$ up to $2.5mA$ at $100K$). The data displayed in Figures 3 and 4 are highly reproducible and do not show any significant hysteretic behavior when the bias current is cycled (5% at its maximum).

We have carefully checked that the Joule heating is irrelevant to account for this current induced effect. The temperature rise of the sample with respect to the sample holder (ΔT) has been measured by attaching a thermometer on the top of the sample itself. We have

obtained $\Delta T \leq 25K$ at the lowest temperature ($80K$) and for the highest power dissipation level. In this low temperature range, the power dissipation level where the NDR sets in leads to $\Delta T \prec 3K$. For higher temperature of measurements, ΔT becomes negligible. Moreover, for these temperatures, the heat dissipation is low which may induce high Joule heating and possible non-linear $V - I$ characteristics. However, at $300K$, $V - I$ curve is linear on the whole current range. Finally, all these points confirm that the phenomenons observed above are not triggered by simple thermal effects or by heating of the crystal.

The $V - I$ characteristics are not strongly modified under magnetic field. As an example, Figure 5 shows measurements at $90K$ with and without magnetic field. It can be observed that the NDR region sets in for rather close values of the current threshold.. The variation is not substantial enough to invoke a magnetic field effect. To sum up, the main results are : (i) Occurrence of a strong non-linear conduction as one approaches T_c leading to NDR when the temperature is lowered well below T_c . (ii) Non-hysteretic $V - I$ characteristics upon cycling the bias current. (iii) No modification of the above features when a magnetic field is applied.

The zero field data shown for $\text{Pr}_{0.8}\text{Ca}_{0.2}\text{MnO}_3$ are reminiscent of M-I transition and non-linear conduction induced by electric field in the CO compounds of the PCMO system ($0.3 \leq x < 0.8$).²⁰⁻²⁵ In the latter experiments, a melting of the CO state is usually invoked to account for this phenomenon. In the case of a current-induced transition, it is proposed that a breakdown of the CO state locally leads to the creation of metallic filaments made up of FM phase when a current threshold is passing through the sample. The resistance drop and, concomitantly, the occurrence of NDR is the result of the current being drawn into the metallic conducting path forming a parallel circuit. Within such a scenario, the experimentally observed disappearance of the NDR upon application of magnetic field is explained by considering the magnetic field induced transformation of AF-COI state into FMM. Coexistence of CO phase and FM one would prevent the nucleation of metallic filaments needed for occurrence of NDR.^{20,22}

Let's now turn to the data obtained for our weakly doped FMI $\text{Pr}_{0.8}\text{Ca}_{0.2}\text{MnO}_3$ crystal.

As developed in Ref.[11] and on the basis of our neutron diffraction data charge ordering is never observed in $\text{Pr}_{0.8}\text{Ca}_{0.2}\text{MnO}_3$. Thus, one can hardly invoke the electric field-induced destabilization of the CO state to understand our experimental data. Our results suggest that for a sufficient bias current, a new conduction path is opened. This conduction path is closely linked to the FM ground state of the sample and magnetic field does not triggers or limit this phenomenon. Moreover, the non-hysteretic nature of the $V - I$ characteristics is not in favor of an electric field-induced metastable state.

Although a theoretical understanding of the mechanisms at work in mixed valent manganites is still incomplete, the DE is commonly adopted as a main ingredient. In the completely ferromagnetic phase, e_g electrons of Mn^{3+} can hop coherently without magnetic scattering by the t_{2g} spins while they become strongly incoherent if the t_{2g} are disordered. However, for ferromagnetic mixed manganites, localization effects can arise due to spatial fluctuations of structural and spin dependent potentials as discussed by Coey et al.²⁷ As emphasized before, in $\text{Pr}_{0.8}\text{Ca}_{0.2}\text{MnO}_3$, the important inward tilt of the $\text{Mn}^{3+} - \text{O} - \text{Mn}^{4+}$ bounds results in a decrease of the e_g bandwidth. An electric field may induce a local electrical moment in the MnO_6 octahedra by modifying the spatial distribution of the charges. This leads to an increase of the $d_{z^2} - p\sigma - d_{z^2}$ overlaps i.e. an increase of the e_g bandwidth. As a consequence, the hopping probability and the mobility of the carriers would be greatly enhance. The magnetic ground state of $\text{Pr}_{0.8}\text{Ca}_{0.2}\text{MnO}_3$ is definitely ferromagnetic, thus there is no need of a magnetic field to initiate a DE-mediated hopping. The slight modification between the $V - I$ curves with and without magnetic field could explained as a field induced suppression of the deviation from perfect collinear ferromagnetism which implies a spin-only moment of $3.8 \mu_B/\text{Mn}$ (Neutron diffraction experiments give $3.46(4) \mu_B/\text{Mn}$ for $H = 0 \text{ Tesla}$). Moreover, this scenario is supported by the temperature dependence of I_{th} . Indeed, the FM correlations are enhanced as the temperature is lowered well below T_c and smaller bias current threshold may be required to induce delocalization via DE.

The non-linear conduction, and more particularly the NDR, can also arise as a result of inelastic tunneling. One can start off from this point by proposing another kind of

process which could be at work in such a low doped system. To do so, one could imagine a rather inhomogeneous material, magnetically speaking. In this scenario, due to the random distribution of the Mn^{3+} and Mn^{4+} ions, the long range FM ordering may appear in spatially distinct regions, strongly topologically disordered, of the sample. In those regions, the DE would be locally at work however metallicity could not be macroscopically observed because these regions, where the carriers are mobile, would be interrupted by tunnel-type weak links, whose nature remains unclear. Twinning might be a clue ; such disorder effects are unavoidable in crystals and could play the role of tunneling junctions between highly ferromagnetic domains. Thus, the peculiar behavior observed in $Pr_{0.8}Ca_{0.2}MnO_3$ can be tentatively understood by considering a spin polarized current flowing across twin-boundary tunnel junctions separating neighboring ferromagnetic domains.

In summary, we have carried out a systematic investigation of the non-linear transport in the FMI $Pr_{0.8}Ca_{0.2}MnO_3$. Experimental data are rather similar to those obtained in charge ordered systems. However, the ground state of $Pr_{0.8}Ca_{0.2}MnO_3$ prevents us to invoke a current-induced destabilization of the charge ordered phase to account for experimental data. We propose interpretations in which the effectiveness of the DE is restored upon application of electric field.

Acknowledgements : The authors thank L. Hervé for crystal growth, G. André and N. Guiblin for preliminary neutron diffraction results and M. Hervieu for electron diffraction characterization.

* : corresponding author

REFERENCES

- ¹ For a review, see *Colossal Magnetoresistance, Charge Ordering and Related Properties of Manganese Oxides*, edited by C. N. R. Rao and B. Raveau (World Scientific, Singapore, 1998) and *Colossal Magnetoresistive Oxides*, edited by Y. Tokura (Gordon and Breach Science, New York).
- ² E. O. Wollan and W. C. Koehler, Phys. Rev. **100**, 545 (1955); J. B. Goodenough, *ibid.* **100**, 564 (1955).
- ³ S. Jin, T. H. Tiefel, M. McCormack, R. A. Fastnacht, R. Ramesh, and L. H. Chen, Science **264**, 413 (1994); R. von Helmolt, J. Wecker, B. Holzapfel, L. Schultz, and K. Samwer, Phys. Rev. Lett. **71**, 2331 (1993).
- ⁴ C. Zener, Phys. Rev. **82**, 403 (1951); P. W. Anderson and H. Hasegawa, *ibid.* **100**, 675 (1955); P.-G. de Gennes, *ibid.* **118**, 141 (1960).
- ⁵ V. N. Smolyaninova, A. Biswas, X. Zhang, K. H. Kim, B.-G. Kim, S.-W. Cheong, and R. L. Greene, Phys. Rev. B **62**, R6093 (2000).
- ⁶ M. R. Lees, J. Barratt, G. Balakrishnan, D. McK. Paul, and M. Yethiraj, Phys. Rev. B. **52**, R14 303 (1995).
- ⁷ M. R. Lees, O. A. Petrenko, G. Balakrishnan, and D. McK. Paul, Phys. Rev. B **59**, 1298 (1999).
- ⁸ Y. Tomioka, A. Asamitsu, H. Kuwahara, Y. Morimoto, and Y. Tokura, Phys. Rev. B **53**, R1689 (1996).
- ⁹ C. Martin, A. Maignan, M. Hervieu, and B. Raveau, Phys. Rev. B **60**, 12 191 (1999).
- ¹⁰ A. Maignan, C. Martin, F. Damay, and B. Raveau, Z. Phys. B **104**, 21 (1997).
- ¹¹ Z. Jiráček, S. Krupička, Z. Šimša, M. Dlouhá, and S. Vratislav, J. Magn. Magn. Mater. **53**, 153 (1985).

- ¹² H. Yoshizawa, H. Kawano, Y. Tomioka, and Y. Tokura, Phys. Rev. B. **52**, R13 145 (1995).
- ¹³ H. Yoshizawa, H. Kawano, Y. Tomioka, and Y. Tokura, J. Phys. Soc. Jpn. **65**, 1043 (1996).
- ¹⁴ Y. Tomioka, A. Asamitsu, Y. Moritomo, and Y. Tokura, J. Phys. Soc. Jpn. **64**, 3626 (1995).
- ¹⁵ A. Anane, J.-P. Renard, L. Reversat, C. Dupas, P. Veillet, M. Viret, L. Pinsard and A. Revcolevschi, Phys. Rev. B **59**, 77 (1999)
- ¹⁶ V. Kiryukhin, D. Casa, J. P. Hill, B. Keimer, A. Vigliante, Y. Tomioka, and Y. Tokura, Nature (London) **386**, 813 (1997).
- ¹⁷ M. Fiebig, K. Miyano, Y. Tomioka and Y. Tokura, Science **280**, 1925 (1998).
- ¹⁸ K. Ogawa, W. Wei, K. Miyano, Y. Tomioka and Y. Tokura, Phys. Rev. B **57**, R15033 (1998)..
- ¹⁹ Y. Moritomo, H. Kuwahara, Y. Tomioka and Y. Tokura, Phys. Rev. B **55**, 7549 (1997).
- ²⁰ A. Asamitsu et *al.*, Nature **388**, 50 (1997).
- ²¹ J. Stankiewicz, J. Sesé, J. García, J. Blasco, and C. Rillo, Phys. Rev. B **61**, 11 236 (2000).
- ²² A. Guha, A. Raychaudhuri, A. Raju and C. N. R. Rao, Phys. Rev. B **62**,5320 (2000)
- ²³ A. Guha, N. Khare, A. Raychaudhuri and C. N. R. Rao, Phys. Rev. B **62**,5320 (2000)
- ²⁴ C. N. R. Rao, A. Raju, V. Ponnambalam, S. Parashar and N. Kumar, Phys. Rev. B **61**, 594 (2000)
- ²⁵ R. C. Budhani, N. K. Pandey, P. Padhan, S. Srivastava and R. P. S. M. Lobo, Phys. Rev. B **65**, 014429 (2001)
- ²⁶ Y. Yuzhelevski, V. Markovich, V. Dikovskiy, E. Rozenberg, G. Gorodetsky, G. Jung, D. A. Shulyatev and Ya. M. Mukovskii, Phys. Rev B **64**, 224428 (2001).

²⁷ J. M. D. Coey, M. Viret, L. Ranno and K. Ounadjela, Phys. Rev. Lett. **75**, 3910 (1995).

I. FIGURES CAPTIONS

Figure 1 : $1.5K$ neutron diffraction patterns : continuous line for calculated plot, stars for experimental data, the upper Bragg strikes correspond to the $Pnma$ crystallographic structure and the lower one are for the magnetic phase. The main indexations are also given. Inset : 020 FM peak intensity versus temperature.

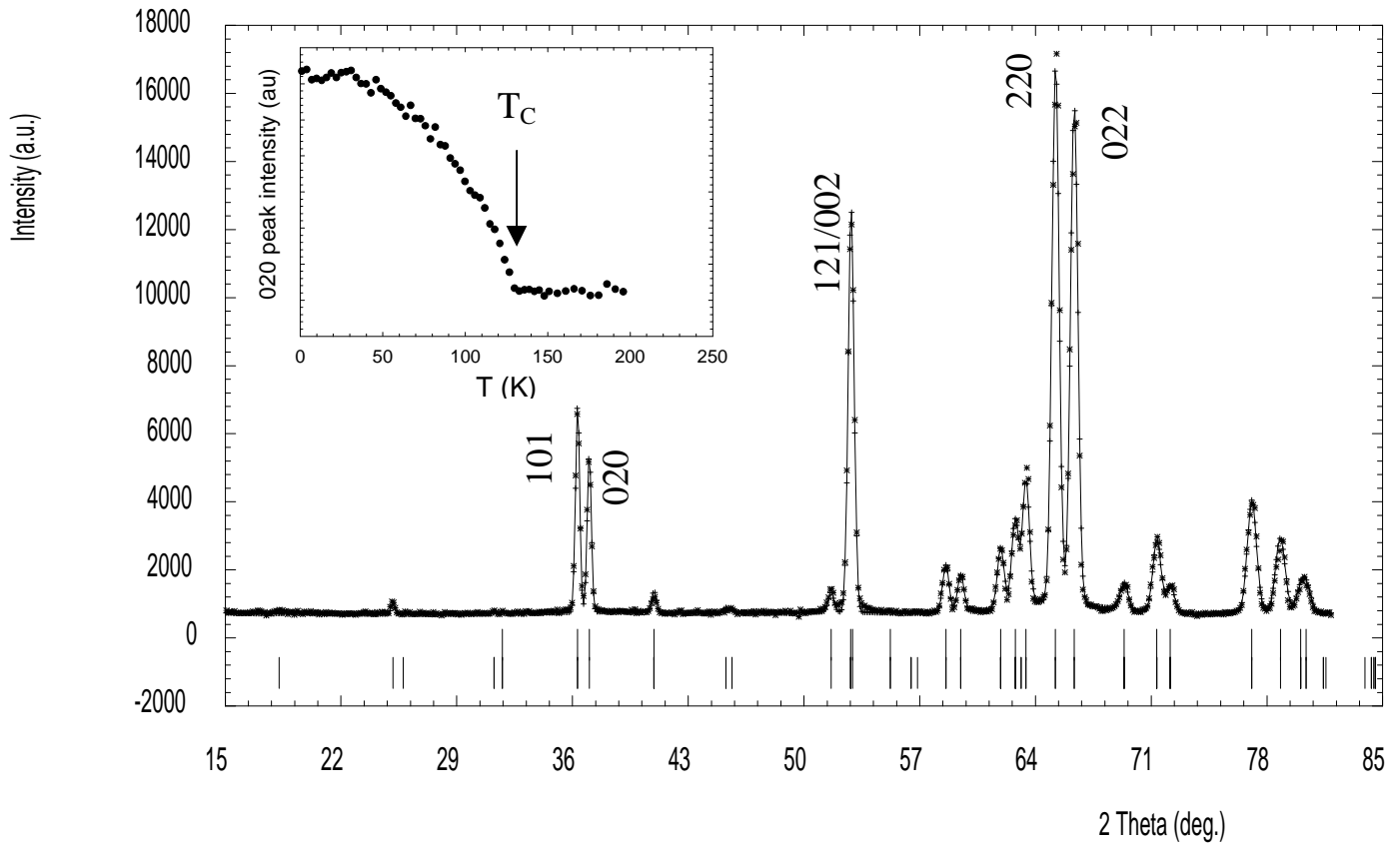
Figure 2 : Temperature dependence of resistance for a $\text{Pr}_{0.8}\text{Ca}_{0.2}\text{MnO}_3$ crystal with various bias currents.

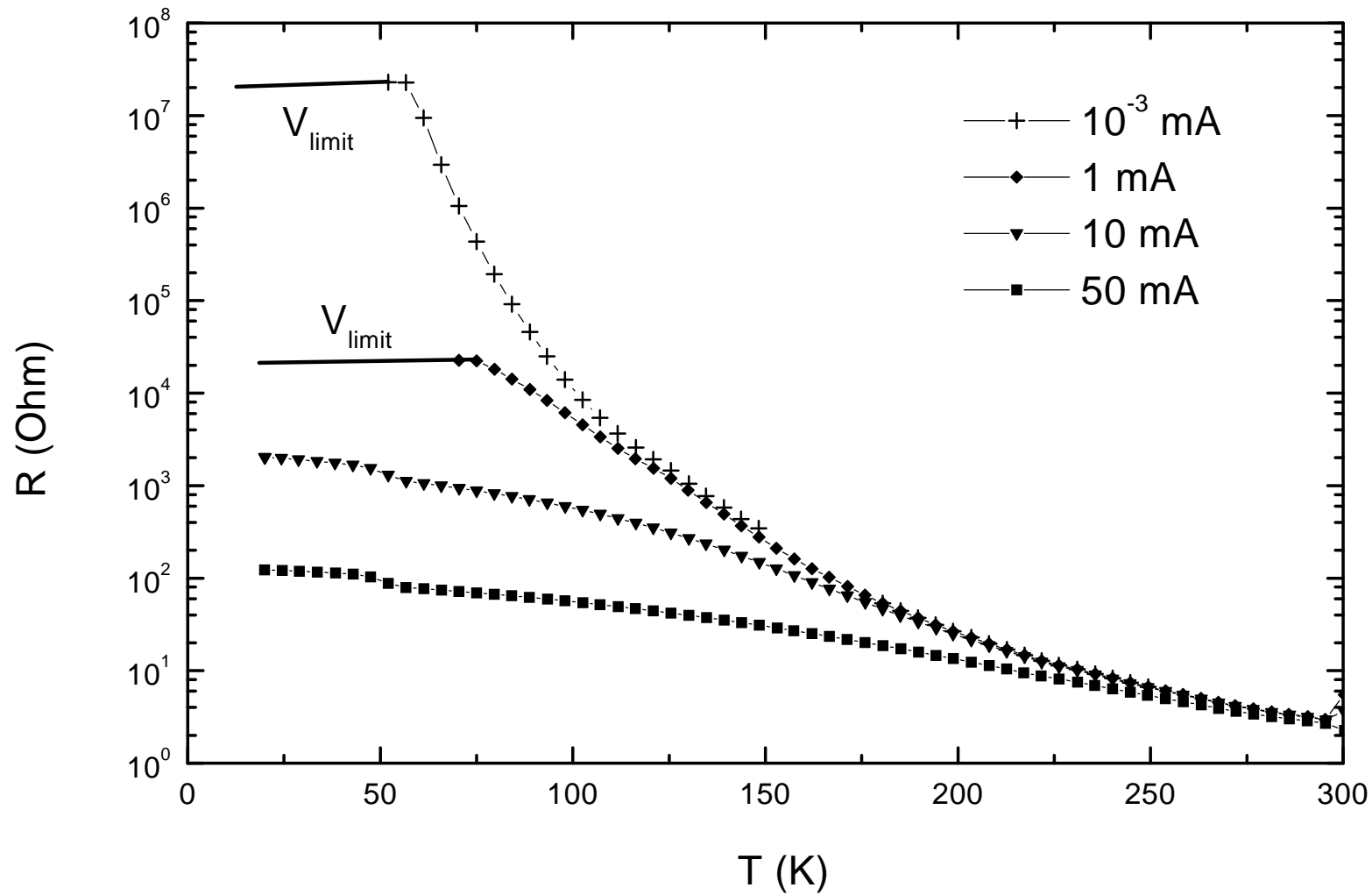
Figure 3 : $V - I$ characteristics under zero field for temperatures below T_c ($80K$, $90K$ and $100K$).

Figure 4 : $V - I$ characteristics under zero field for temperatures above T_c ($170K$ and $300K$).

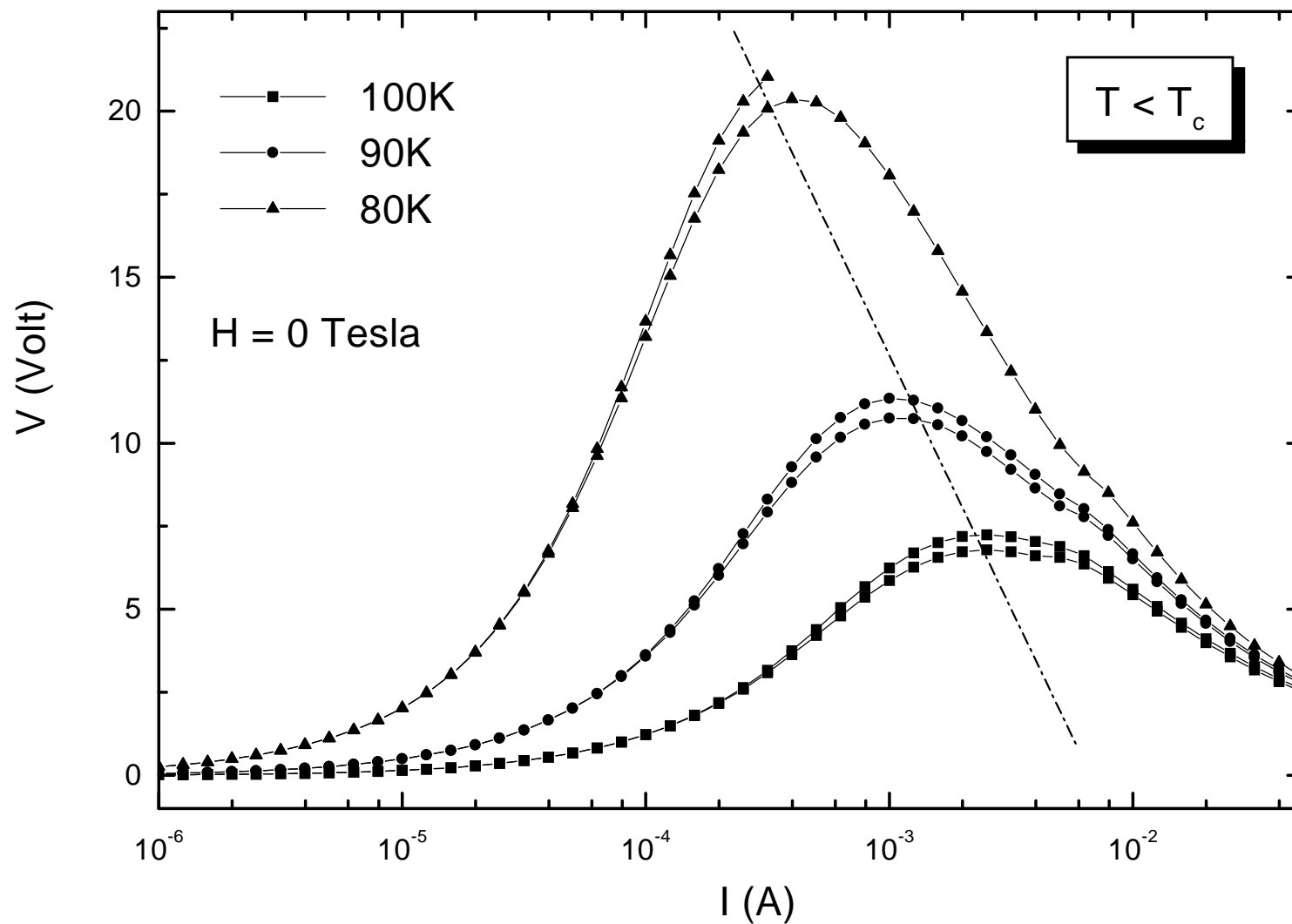
Figure 5 : $V - I$ characteristics for $T = 90K$ under 0 and 8 Tesla.

Pr_{0.8}Ca_{0.2}MnO₃ 1.5K





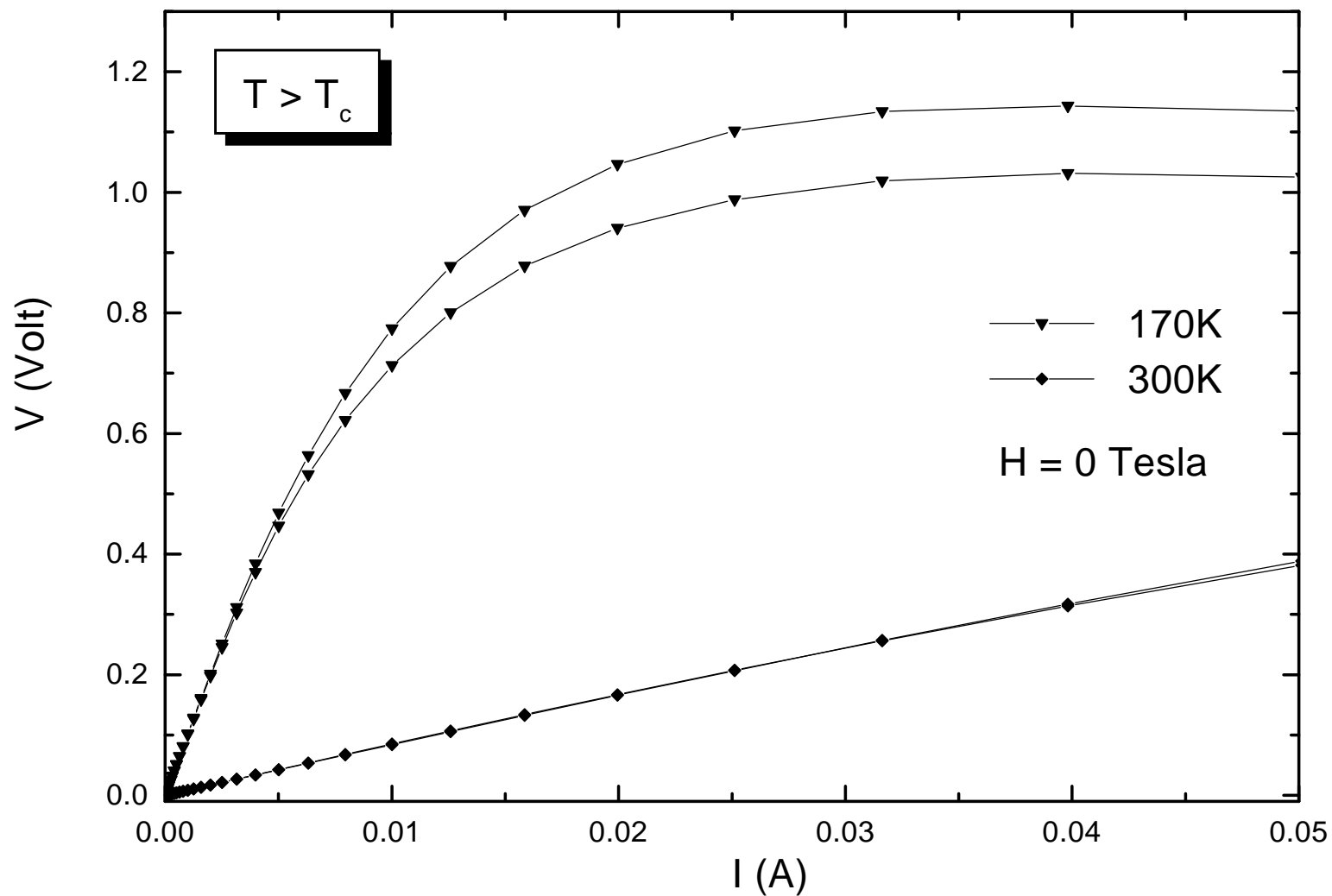
A. Wahl et al.
Physical Review B
Figure 2



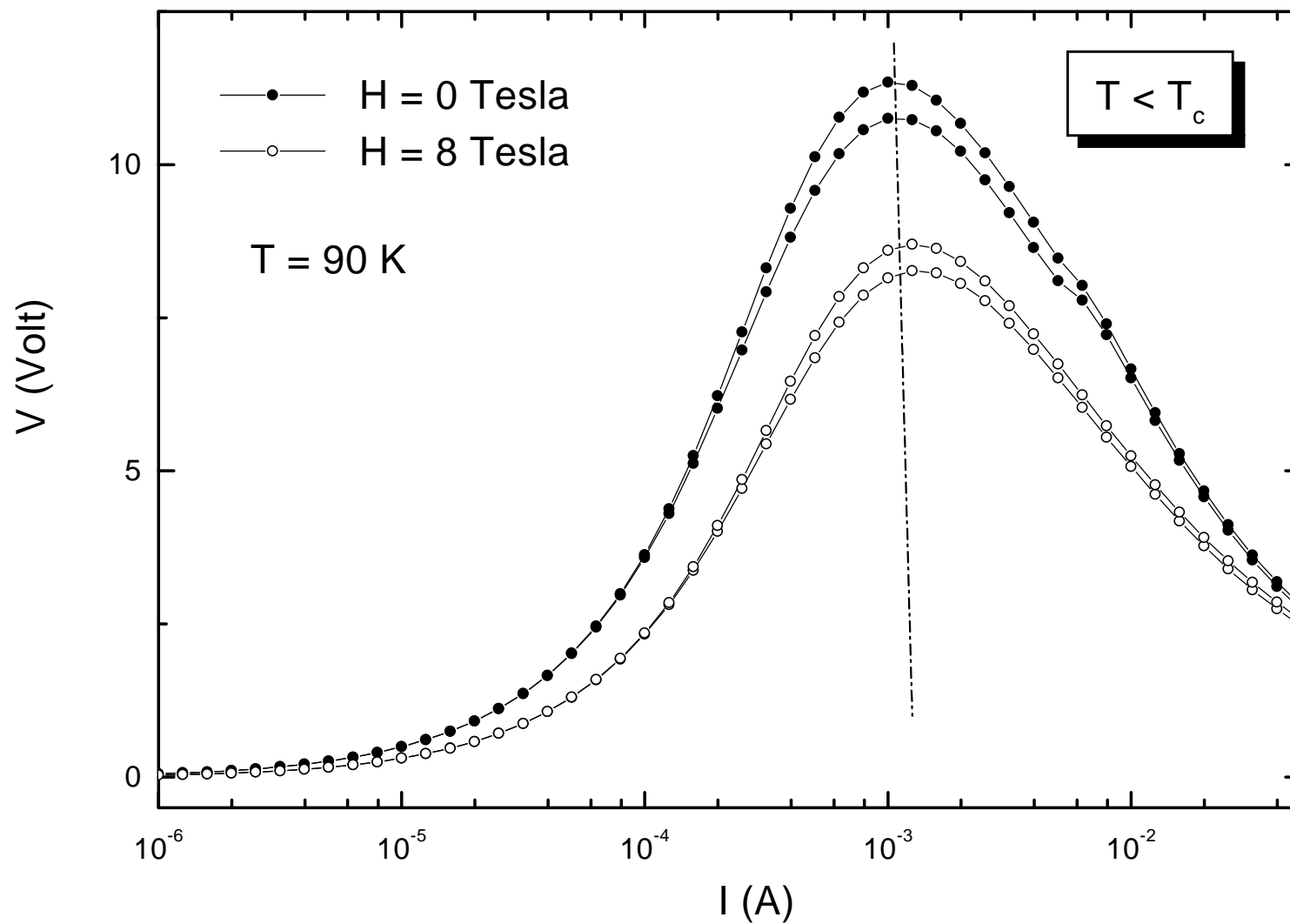
A. Wahl et al.

Physical Review B

Figure 3



A. Wahl et al.
Physical Review B
Figure 4



A. Wahl et al.
Physical Review B
Figure 5